DEFORMATION OF TUNNEL IN SOFT GROUND DURING EARTHQUAKE

C. Tamura (I)
S. Okamoto (II)
K. Kato (III)
Y. Kido (IV)
Presenting Author: C. Tamura

SUMMARY

The deformations of tunnels during earthquakes are described based on the results of earthquake observations at a submerged tunnel, shield tunnels, and box-section tunnels constructed in soft ground. It is found that strains in the axial direction of a tunnel are produced by the behaviors of the surface ground and of the bedrock, and that the deformation of the tunnel cross section is mainly produced by shearing deformation of the surface ground, and also by the behavior of the bedrock.

1. INTRODUCTION

In contrast to structures above ground being designed for earthquake resistance by the seismic coefficient method based on inertia forces, it has become common for earthquake-resistant design of underground structures to be made by the displacement method computing stresses and strains on causing the structures to be displaced statically according to the displacement of the surrounding ground during earthquake. In order to expand this design method rationally, it is necessary to accumulate data concerning behaviors of actual structures during earthquakes.

The authors have been carrying out continuous earthquake observations at five locations in actual tunnels of three kinds in Tokyo and its vicinity. More than 100 earthquakes have been recorded so far, and since a number of new facts have been learned concerning axial and cross-sectional deformations of tunnels during earthquakes, these will be reported here.

2. OUTLINES OF GROUND AT OBSERVATION POINTS AND CONDITIONS OF INSTRUMENT INSTALLATION

The observation sites were one location at Tamagawa Tunnel (previously called Haneda Tunnel) on the Keiyo Line of the Japanese National Railways (hereafter called KT Ob-Point), two locations (ST Ob-Point, SN Ob-Point) in shield-driven tunnels (hereafter called shield tunnels) for an underground railroad, and two locations (BS Ob-Point, BH Ob-Point) of two-track, box-section underground railroad tunnels, for a total of five points.

(I) Professor, Institute of Industrial Science, University of Tokyo, Tokyo, Japan
(II) Professor Emeritus, University of Tokyo
(III) Research Fellow, Institute of Industrial Science, University of Tokyo
(IV) Research Engineer, K.K. Kumagai-gumi, Tokyo, Japan

1) The KT Ob-Point is at a submerged tunnel crossing the bottom of the Tama River near its mouth and is composed of six elements of egg-shaped cross section each of height of 8.8 m, width of 13 m and length of 80 m, a total of 480 m, and the joints between elements and with ventilation towers are rigid connections. The thickness of the alluvial layer at the surface is 35 - 40 m at the thalweg, and around 15 m at both banks. Underneath, there is a diluvial sand-gravel layer of N-value higher than 50 (at the thalweg) or diluvial silt layers of N-value 10 to 20 (at both banks) (Fig. 1). The measuring instruments are accelerometers and strain gages, at four points on the tunnel axis, 0 m, 30 m, 125 m, and 50 m successively apart, on both side walls in the axial direction of the tunnel for a total of eight strain gages installed (Ref. 1).

2) The tunnel cross section of SN Ob-Point is as shown in Fig. 2, and is composed of reinforced concrete segments of width of 90 cm. Besides three-component accelerometers, 13 strain gages from SA-SO-1 to ST-SI-13 are installed. The first two letters in the identifications of the strain gages, SA or ST, indicate the strains of the tunnel walls in the axial direction of the tunnel and in the transverse cross-sectional plane, while the numbers at the ends indicate the changes (strains) inside the segments if odd numbers, and the changes between marked points sandwiching joints between segments if even numbers. (Hereafter, the strain gages are called Gage 1, Gage 2, etc., taking the numbers at the ends.)

   The surface layer of 10 m at these observation points is Kanto loam of N = 2 - 5, underlying which is a sand layer of N = 25 to 40 or more, the tunnel having been constructed at a depth of approximately 13 to 19 m. In order to observe the relative movements between tunnel and ground, three-component accelerometers are buried in the ground at the sides of the tunnel.

3) The tunnel cross section at ST Ob-Point is practically the same as that at SN Ob-Point, and the installation of instruments and identifications are also similar. However, a Gage 13 is not installed at this observation point. Also, seismometers have been installed in the ground. At this point, the layer down to 36 m from the ground surface is a silty clay of N = 2 to a depth of 29 m, and N = 5 from 29 m to 36 m. From 36 m to 52 m is a sand-bearing clayey silt of about N = 10, underlying which is a consolidated Tokyo Sand-Gravel Layer of N = 50 and higher. The tunnel has been constructed at a depth of approximately 11 to 17 m.

4) The cross section at BS Ob-Point and the condition of instrument installation there is as shown in Fig. 3. The third letters in the identifications, A and S, indicate acceleration and strain, respectively, while of the letters at the end, A and V respectively indicate axial direction and vertical direction of the tunnel, P and T respectively indicate values measured in the horizontal direction perpendicular to the tunnel axis, and in the transverse cross section of the tunnel. Accelerometers are buried in the ground to the side of the tunnel. In order to observe the relative movements of the tunnel and ground, a three-component accelerometer is buried in the ground at the side of the tunnel. The outline of the surface layer ground of this observation point is that down

to a depth of 2 m is topsoil, down to 7 m is a silty, sandy soil of about N = 2, underlying which there is humus of thickness of 1 m and N = 6. Down to 12 m is a sandy soil of N = 6 - 9, under which there is silt of N = 5 - 6 down to 50 m. The ground deeper than 50 m is a diluvial layer with a sandy soil of N-value higher than 50 down to 62 m, subjacent to which there is a Tokyo Sand-Gravel Layer of N-value higher than 50. The tunnel has been constructed at a depth of 13 - 19 m from the ground surface.

5) The cross section at BH Ob-Point is roughly similar to that at BS Ob-Point, with instruments given similar identifications as in 4) above. At this observation point the surface layer of approximately 5 m is topsoil, underlying which is hard mudstone, the tunnel having been constructed in this mudstone layer. Accelerometers in the ground are installed at depths of 1 m and 14 m from the ground surface.

3. NATURES OF STRAINS IN TUNNELS DETERMINED FROM OBSERVATIONS

It is a widely known fact that strains of a tunnel during earthquake are produced by displacements during earthquake of the ground surrounding the tunnel. It is not an easy matter to grasp the movement of ground during an earthqauke, including the direction of depth over a wide area, and because of this, studies by model experiments are being made. Accordingly, the results of earthquake observations are important for grasping the earthquake-resistant design of the tunnel and the behavior of the ground during earthquake from an engineering standpoint. The information obtained from observations will be described here.

3.1 Strains in Axial Direction of Tunnel

The results of observations being carried out at KT Ob-Point since 1970 have been reported regarding strains in the axial direction of the tunnel produced in the tunnel walls during earthquakes (Ref. 1). Figure 4 shows the relation between maximum axial strain observed at the tunnel and the epicentral distance with magnitude as the parameter. This is a figure previously reported in which slight changes have been made adding the principal ones from among subsequently obtained data. Figure 5 shows the relation between maximum acceleration in the horizontal direction and the maximum axial strain recorded in the tunnel with magnitude as the parameter. The black dots in the figure are values observed at KT Ob-Point with the regression line drawn based on these. As for the symbols x, o, Δ, and $\otimes$, they indicate observed values at the observation points ST, SN, BS, and BH. Further, the numerals added to these symbols indicate the magnitudes of the earthquakes. In Figs. 4 and 5, the black dots with "A" added are strain waveforms recorded simultaneously which indicated especially large values. This is because it can be judged that there was influence of abrupt variation in the dynamic properties of the surface layer ground. In consideration of the structural characteristics of the shield tunnel, the average of the strains of the segment itself and the strains between marked points including joints between segments is taken as the strain of the shield tunnel.

The following are learned from these figures:

i) The maximum strain in the axial direction of the tunnel at KT Ob-Point is greatly affected by the magnitude of the earthquake.

ii) That maximum strain increases proportionately to approximately the 0.6 power of the maximum acceleration inside the tunnel.

iii) The relation of maximum strain and magnitude with epicentral distance may be approximately expressed by the empirical formula below, although there is a trend of increase in the rate of increase as the epicentral distance is approached.

$$\log_{10} \varepsilon_m = 0.7M - \Delta/450 - 3.2$$

where, ε_m: maximum strain in axial direction ($\times 10^{-6}$)
M: magnitude of earthquake
Δ: epicentral distance (km)

iv) Regarding the ST, SN, and BS observation points, sufficient data have not yet been obtained, but it is assumed that properties roughly similar to the observation results of KT Ob-Point are possessed.

v) The strains at BH Ob-Point are extremely small compared with those at the other observation points. This is thought to be because the ground in which embedment was done was extremely hard compared with the other observation points and displacement and deformation during earthquake were small compared with the others.

As described above, in case of a shield tunnel, it was found that there is a considerable difference between strains of segments and average strain between marks including joints depending on the earthquake motion. Figure 6 shows a record for ST Ob-Point (M = 6, Δ = 41 km, February 27, 1983), which is an example of a record indicating such a property.

The maximum strains at Gages 1, 2, 5, 6, and 10 in the figure are 7.15 μ, 22.89 μ, 7.27 μ, 26.03 μ, and 15.83 μ, respectively. On averaging Gages 1 and 2, and Gages 5 and 6, which are at the same locations, the values are 15.02 μ and 16.65 μ, and agree well with Gage 10. When strains are in the range of several microns, such differences cannot be seen between the indications of strain gages at the same locations, but there is a trend for the differences to become conspicuous as strains become larger. This indicates that joints between segments have the function of absorbing strains of the tunnel.

It has been reported that the sizes of axial strains of a tunnel are related to variations in dynamic characteristics of the ground, frequency characteristics of input waveforms, and natural frequency of the ground (Ref. 1). It was also reported that strain waveforms seen to be produced by surface waves were observed (Ref. 1). Here, as an example of deformation in the direction of the tunnel axis, the strain record at KT Ob-Point in the 1978 Izu Oshima Kinkai Earthquake will be cited.

3.2 Deformation of Tunnel Cross Section

In case of studying deformations of a tunnel cross section, when rigidity

of the cross section is considered, it will be suitable to take the observation points of BS, BH, SN, and ST as objects.

3.2.1 Deformation of Shield Tunnel

A typical earthquake record obtained at a shield tunnel is shown in Fig. 8 (SN Ob-Point, M = 5.4, Δ = 34 km, September 24, 1980). As can be seen in this figure, strain waveforms for Gages 7, 8 and 13 are very predominant, Gages 7 and 8 are of identical phases while Gage 13 is of reverse phase, and the temporal variations in amplitudes of these are very similar to the temporal variations in amplitudes of acceleration waveforms. In view of the above, it is thought that the cross section has changed as shown in Fig. 9(a).

Figure 10 is a record obtained at ST Ob-Point in the Izu Oshima Kinkai Earthquake of 1978. Gages 2, 9 and 10 show axial strains, and it can be seen they are very similar to the strain waveforms of KT Ob-Point shown in Fig. 7. However, on looking at the waveforms of Gages 3, 4, 7, 8, 11, and 12, those for Gages 3, 4, 11, and 12 are quite similar with regard to both size and phase, while those for Gages 7 and 8 are different regarding both phase and size, and what is especially important is that the sizes are smaller compared with the case of Fig. 8.

Such a relation appears in case of an earthquake in which components of comparatively long periods of several seconds are predominant. The deformation of the cross section in this case differs from that in Fig. 9(a) and is considered to be as shown in Fig. 9(b).

Figure 9(a) is a case of the dynamic characteristics of the surface ground having appeared prominently, while Fig. 9(b) is estimated to have been produced by wave motions of long periods propagated through the basement. Incidentally, the distance between the two observation points of KT and ST is approximately 16 km.

3.2.2 Deformation of Box-shaped Tunnel Cross Section

Figures 11 and 12 show parts of the records of BH Ob-Point (M = 5.7, Δ = 107km, March 7, 1982) and BS Ob-Point (M = 6.0, Δ = 41km, February 7, 1983).

On comparisons of the strain waveforms at both side walls in the transverse cross section and the strains in the axial direction of the tunnel in Fig. 11, that the strains of the top slab and the two side walls in the transverse cross section are double to triple in size, further, that the strain waveforms of the two side walls in the transverse cross section are geometrically similar can be recognized. It can be seen that the absolute value of the strain in the top slab compared with the absolute values of strains at the two sides is slightly on the small side, while the phase deviates by 180 deg. This indicates that the tunnel cross section was deformed during the earthquake.

The same trend as in Fig. 11 can be seen in Fig. 12, but what is especially noteworthy is that the strain in the top slab is large compared with others.

The deformations described above may be considered to have been produced because the tunnel cross section is a box-shape of rigid connections.

CONCLUSIONS

The deformations of tunnels in soft ground during earthquakes in their axial directions and in their cross sections were investigated through earthquake observations on a submerged tunnel, box-section tunnels, and shield tunnels. As a result, it has been found out that cross-sectional deformation is mainly produced by the dynamic behavior of the surface ground, with the deformation ordinarily being due mainly to horizontal motion, but with a box-section tunnel strains are produced by vertical motions also. As for the axial directions of tunnels, deformation is produced mainly by the behavior of the surface ground during earthquake, but it has been found that the deformation is also produced by deformation of the basement during earthquake.

In closing, the authors wish to express their sincerest gratitude to the Teito Rapid Transit Authority for its assistance and cooperation in carrying out this study.

REFERENCES

1. C. Tamura, S. Okamoto, and K. Kato: "Earthquake Observations on Tunnels in Soft Ground," Proc. of 5th Japan Earthquake Engineering Symposium, 1978.

2. C. Tamura, K. Kato, K. Yuyama, and Y. Kido: "On Twisting Deformation of Tunnels in Soft Ground During Earthquakes," 16th Earthquake Engineering Research Meeting of JSCE, July 1981.

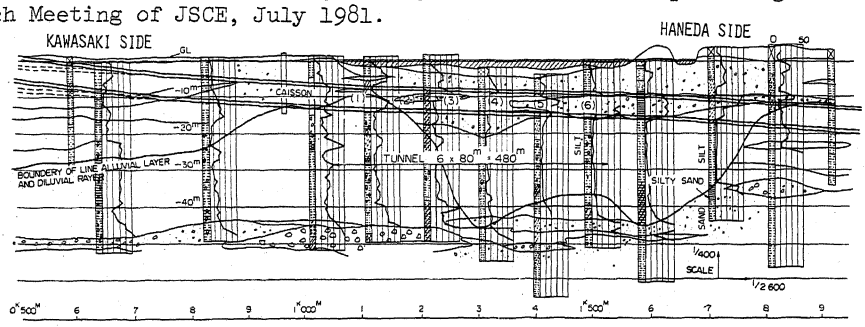

Fig. 1 GEOLOGICAL MAP OF THE SITE OF THE TAMAGAWA TUNNEL

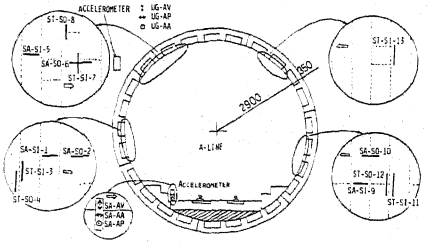

Fig. 2 CROSS-SECTION OF TUNNEL AND INSTRUMENTS AT SN Ob-Point

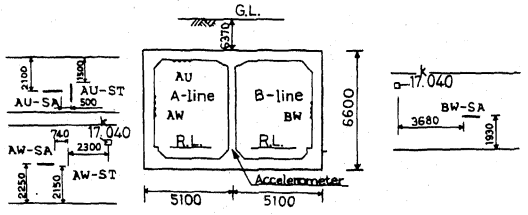

Fig. 3 CROSS-SECTION OF TUNNEL AND INSTRUMENTS AT BS Ob-Point

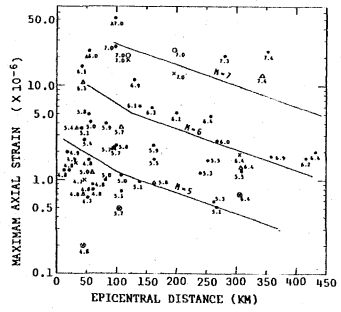

Fig. 4 RELATION BETWEEN MAXIMUM AXIAL STRAIN OF TUNNEL AND EPICENTRAL DISTANCE

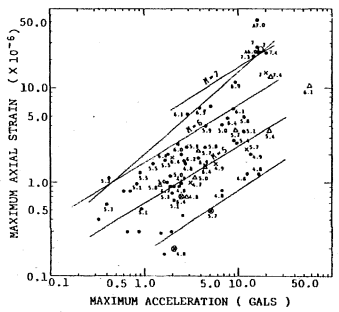

Fig. 5 RELATION BETWEEN MAXIMUM AXIAL STRAIN AND MAXIMUM ACCELERATION

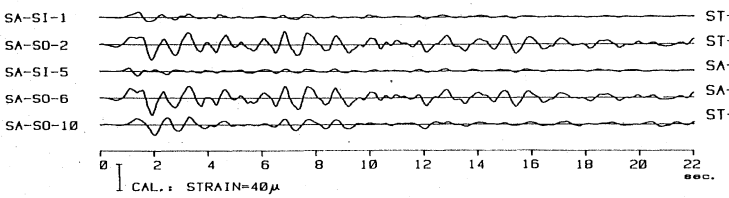

Fig. 6 AXIAL STRAIN OF SEGMENT AND AVERAGE AXIAL STRAIN OF MEASURING LENGTH OF SEGMENT-JOINT-SEGMENT AT ST Ob-Point

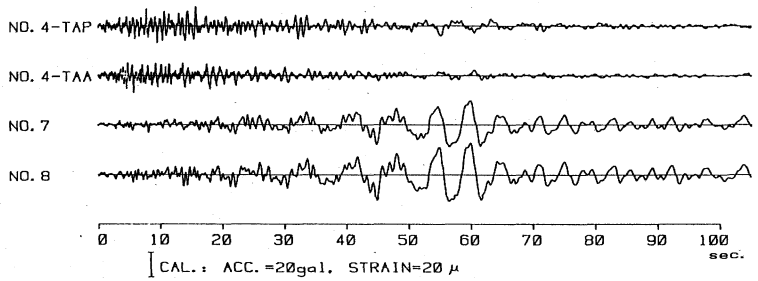

Fig. 7 EARTHQUAKE RECORD OF 1978 Izu-Oshima Kinkai Earthquake AT KT Ob-Point

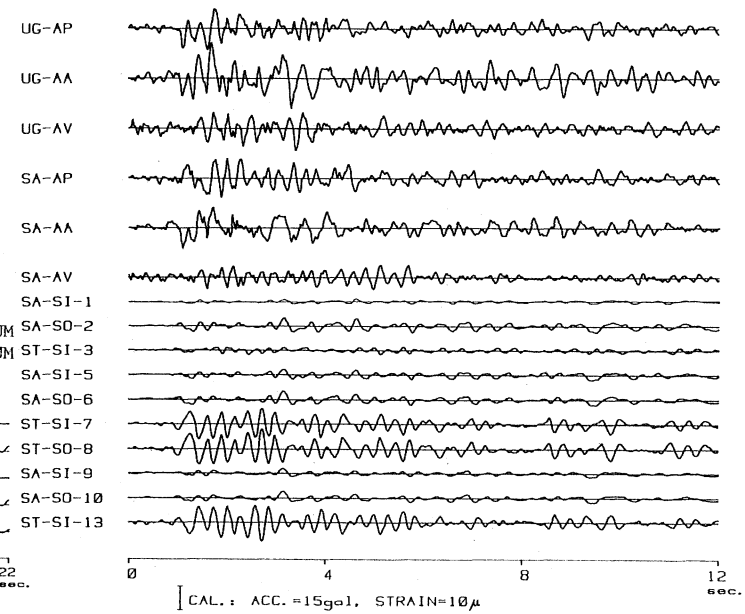

Fig. 8 EARTHQUAKE RECORD AT SN Ob-Point (M=5.4,Δ=34km,Sep.24,1980)

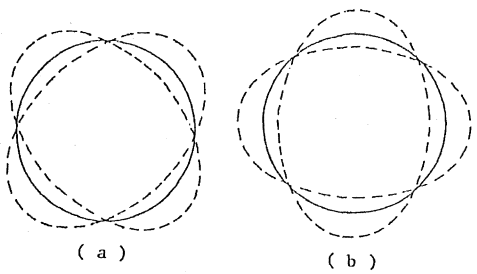

Fig. 9 TYPICAL DEFORMATION OF CROSS-SECTION OF SHIELD TUNNEL DURING EARTHQUAKES

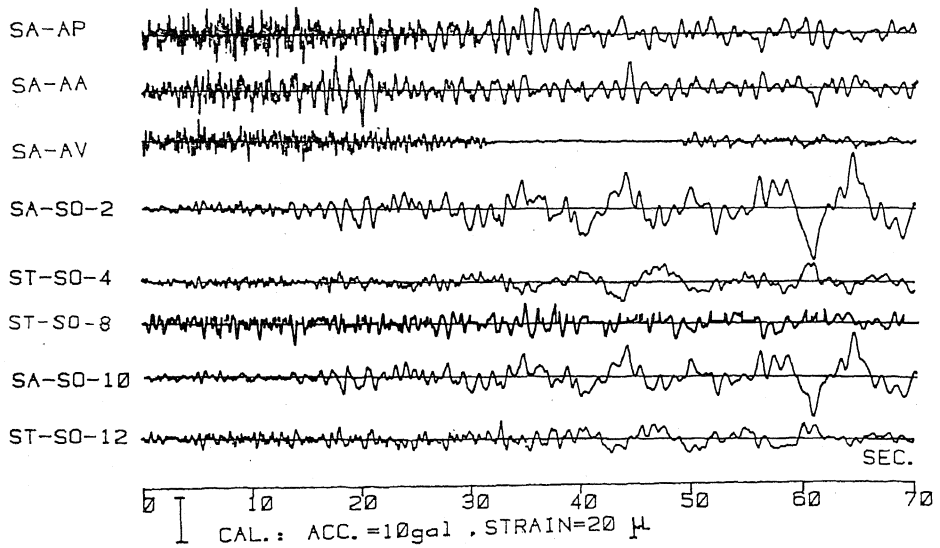

Fig. 10 EARTHQUAKE RECORD OF 1978 Izu-Oshima Kinkai Earthquake AT ST Ob-Point

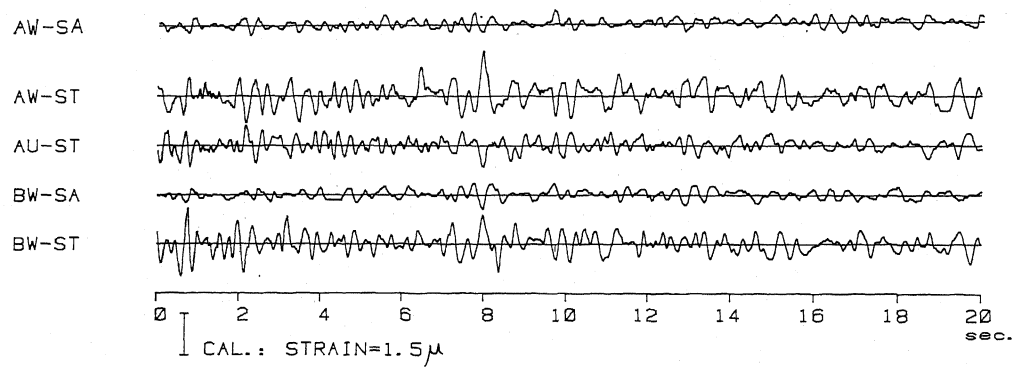

Fig. 11 EARTHQUAKE RECORD AT BH Ob-Point (M = 5.7, Δ = 107km, March 7,1982)

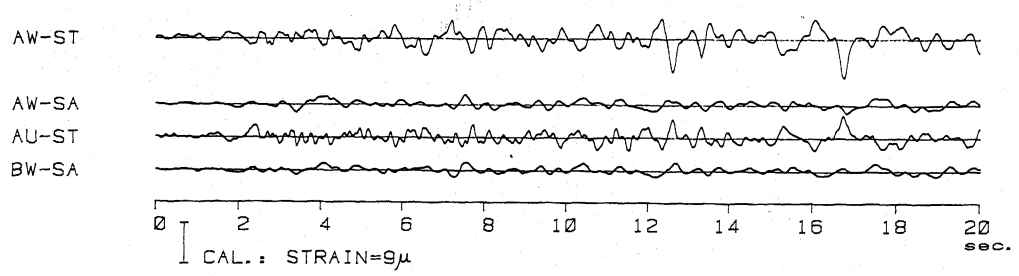

Fig. 12 EARTHQUAKE RECORD AT BS Ob-Point (M = 6.0, Δ = 41km, Feb. 7, 1983)